**Western Region Technical Attachment**
**No. 92-23**
**June 24, 1992**

# THE DEVELOPMENT AND EVOLUTION OF FLASH-FLOOD-PRODUCING THUNDERSTORMS OVER SOUTHERN NEVADA ON AUGUST 10, 1991

**Tom Cylke - Lead Forecaster WSFO Reno**

## INTRODUCTION

A sequence of events and several meteorolgical parameters are examined which led to the development of flash-flood-producing thunderstorms over southern Nevada on August 10, 1991. GOES enhanced infrared imagery along with lightning and radar data were primarily used to depict the sequence of thunderstorm development. The use of a 700 mb equivalent potential temperature (theta-e) analysis provides further insight as to the redevelopment and propagation of the thunderstorms later in the evening when flash flooding occurred. The heavy rain that occurred in the Las Vegas area around 9:20 PM PDT resulted in mostly local street flooding and fortunately no fatalities, although some motorists had to be rescued from rising water. This study emphasizes the importance of pattern recognition, topography and convective scale interaction when forecasting or analyzing thunderstorm development under a weak synoptic flow pattern.

## SYNOPTIC SCALE ENVIRONMENT - PATTERN RECOGNITION

The evolution of deep convection over southern Nevada on August 10, 1991 was primed by a synoptic environment which led to a moist and unstable airmass. The pattern was very similar to the classic flash flood pattern for a Type 2 deformation event (Spayd, 1986) (Fig.1) where a weak 500 mb low was located over the northern Gulf of California (Fig.2) and an upper level trough was moving across the Pacific Northwest. A surface thermal trough along with a 700 mb deformation zone (Figs. 3,4) were analyzed over southern Nevada contributing to the overall low-level convergence, contributing to an upward vertical motion field.

## CONVECTIVE SCALE INTERACTION- SEQUENCE OF EVENTS

Satellite imagery during the afternoon of August 10, 1991 (Fig.10) shows convection to be highly terrain-dependent over Arizona and Nevada as is typical with weak synoptic forcing in the summer (Hales, 1991). Recent studies using regression analysis of lightning data and forecast NGM fields show a primary prerequisite for the formation of thunderstorms to be large scale static instability followed by a secondary contribution from local convergence in the wind and moisture fields (Reap, 1991). In areas of weak dynamic forcing, thunderstorms will form over higher terrain as differential heating results in upslope flow (Purdom, 1986). During the early afternoon hours of August 10, 1991 convective clouds were developing over the higher terrain of northwest Arizona and southern Nevada. Both satellite and lightning detection data indicated a large area of thunderstorms over the northwest plateau of Arizona by afternoon. The subsequent

formation of a large "bubble" surface high formed by rain-cooled outflow was critical in developing a convergent wind pattern over southern Nevada later Pat evening. The anticyclonic flow associated with this rain-cooled surface high is evident in the surface geostrophic wind analysis later that evening (Fig.5). Besides the satellite sequence (Figs. 10,11,12,) the sequence of radar (Figs.6,7) and lightning detection graphics (Figs.8,9) also showed thunderstorms over the higher terrain of northwest Arizona and southern Nevada during the late afternoon hours, redeveloping into the lower elevations of southern Nevada during the evening hours. The 64 strike maxima on the lightning detection graphic at 0245Z (Fig.9) just east of Las Vegas preceded the reported flash flooding in that area by about an hour.

**IMPORTANCE OF THETA-E ANALYSIS**

Equivalent potential temperature (theta-e) is a thermodynamic property dependent on moisture and temperature, whereby higher values are often indicative of more available thermal energy in the form of CAPE (convective available potential energy). CAPE accounts for both sensible and latent heat available for convection. The theta-e ridge axis most often lies in the overlapping area between the thermal ridge and the moisture ridge. Recent observations and studies (Scofield, 1990) suggest that organized convective systems will often propagate toward theta-e maxima feeding off the available potential energy.

It is no coincidence that the theta-e analysis (run on the PC-THETAE program (Last, 1991)) at OOz August 11,1991 showed a theta-e maxima over southern Nevada (Fig. 13). The evolution of this theta-e maxima over southern Nevada can be partly, if not mostly, attributed to strong solar heating under mostly clear skies during the day. In fact, it is interesting to compare the satellite imagery from the afternoon of August 10th (Fig.10) with imagery later that evening (Fig.12). The areas which were cloud-free over southern Nevada during the afternoon became the most cloudy areas during the evening hours as thunderstorms propagate and redevelop into the high theta-e area.

Gust fronts or outflow boundaries occur with virtually all convective storms and in all directions, however only some persist and redevelop new thunderstorms. These new thunderstorms will likely occur where outflow boundaries intersect other boundaries in regions where sufficient instability exists.

Theta-e analyses when combined with satellite imagery have been shown to be an important tool in assessing thunderstorm development and propagation, and proved to be exceptionally accurate over southern Nevada on the evening of August 10, 1991.

**CONCLUSIONS AND SUMMARY**

1) Given a large area of static instability (i.e. lifted index values of zero or less) with weak dynamic forcing, thunderstorms will form initially over higher terrain where differential heating results in upslope flow.

2) Thunderstorms will most likely propagate or redevelop into cloud-free areas of high

instability (often theta-e ridges).

3) Merging outflow boundaries are the primary focusing mechanism for thunderstorm redevelopment under weak synoptic flow patterns.

4) In areas of sparse surface observation such as the desert south- west, satellite and lightning detection are invaluable in detecting outflow boundary development. The network of upper air and surface observations in the desert southwest is entirely inadequate for any true mesoanalysis (Doswell, 1982). In recent years, satellite iniagery and lightning data have led to a new understanding of convective detection and development. Hopefully, new technology (such as Doppler radar, ASOS, and better surface meso-networks) will provide even more insight and forecast lead-time of these mesoscale features.

**REFERENCES**


Doswell,C.A.,1982: The operational meteorology of convective weather, volume I: operational mesoanalysis. NOAA Technical Memorandum NWS NSSFC-5

Hales,J.E.,1991: Terrain influence on Arizona thunderstorms during the summer monsoon: A case study during SWAMP 1990. NSSFC Operational Notes, October 1991

Last,J.K,1991: PC-THETAE. CRCP-9MC, August 1991

Purdom,J.,1986: Satellite contributions to convective scale weather analysis and forecasting. Preprints, 11th Conference on Weather Forecasting and Analysis, 295-314.

Reap,R.M.,1991: Climatological characteristics and objective prediction of thunderstorms over Alaska. Weather and Forecasting,6, 309-319.

Scofield,R.,1990: Patterns of low level theta-e ridge axes and maxima associated with the development and propagation of organized convection. Graphical Guidance, 1991, NWSTC, 126-136

Spayd,L.E.,1986: Detecting and forecasting western region flash floods using GOES imagery and conventional data. Preprints, 11th Conference on Weather forecasting and Analysis, 315-320.

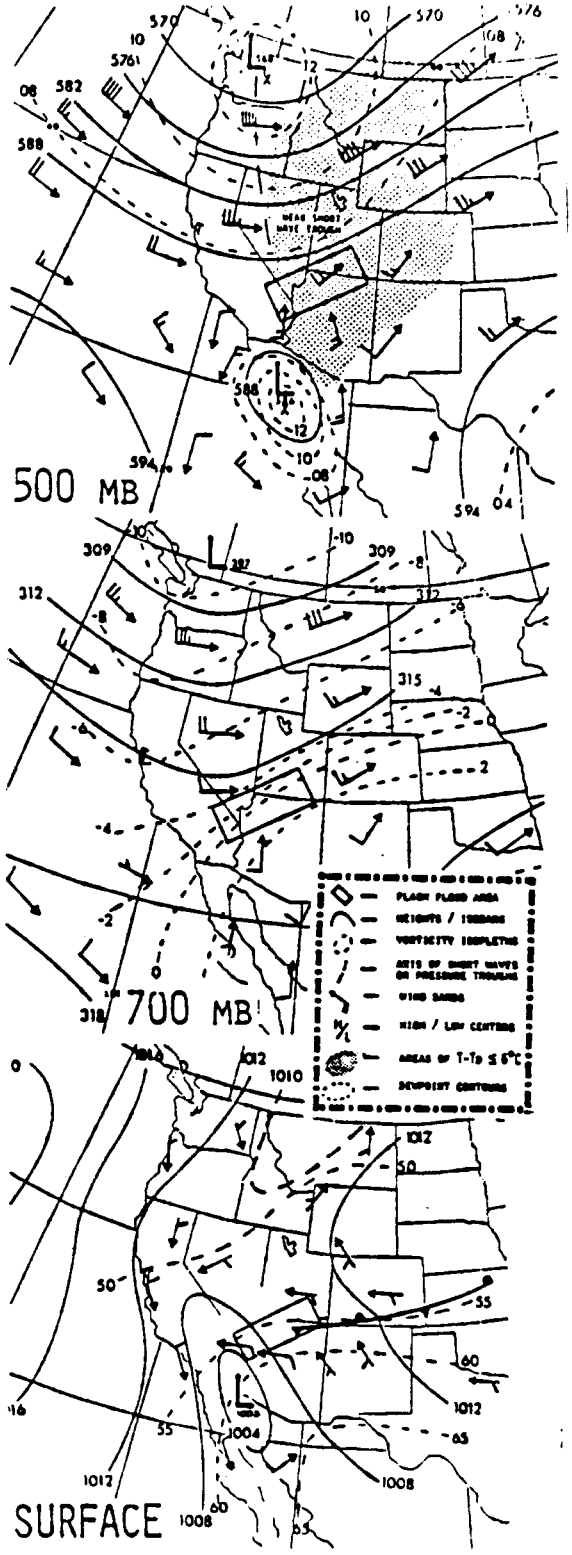


Figure 1 Atmospheric Composites for the Type 2 Deformation Zone events.

FIG.1

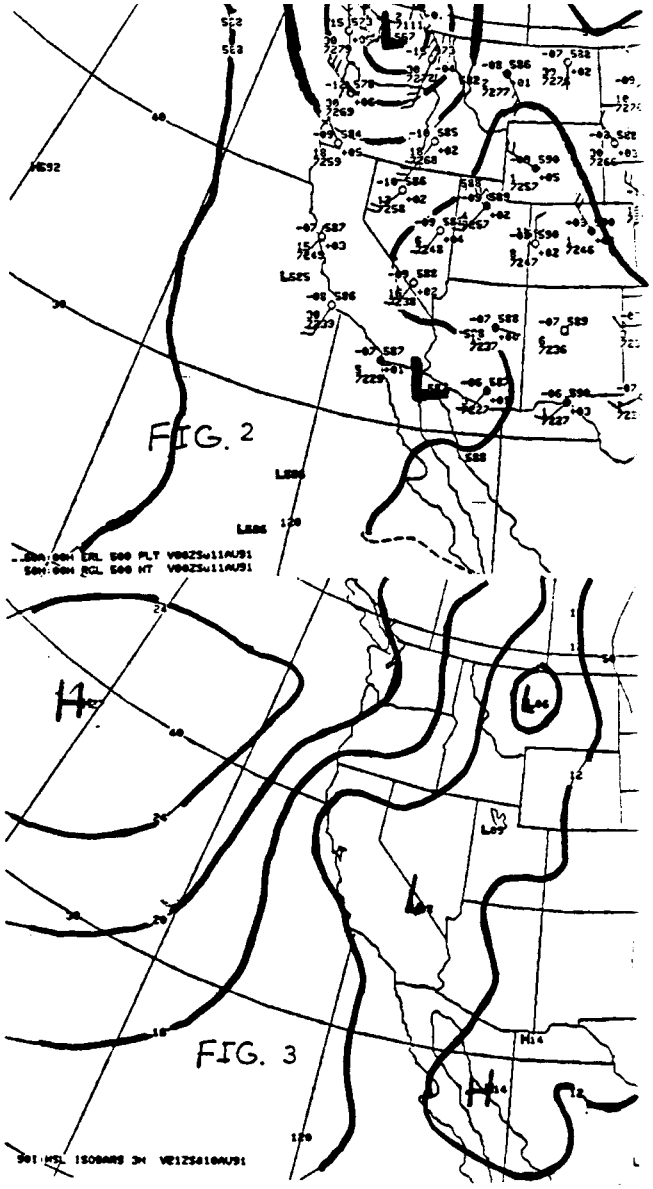

FIG. 2

FIG. 3

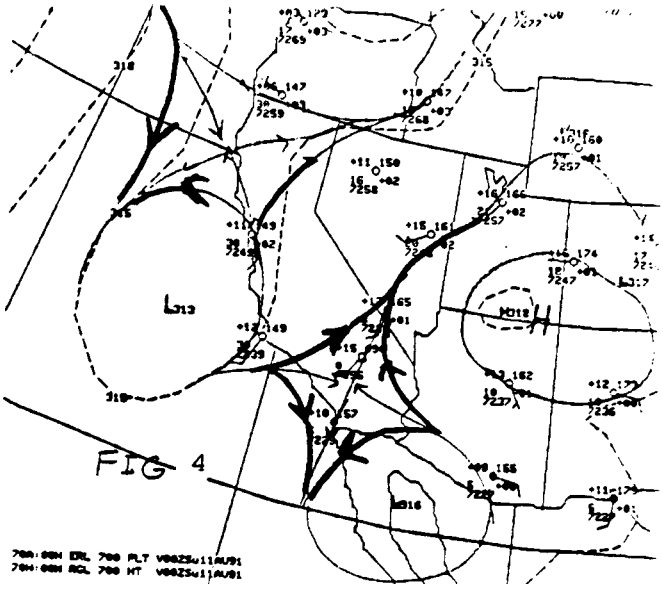

FIG 4

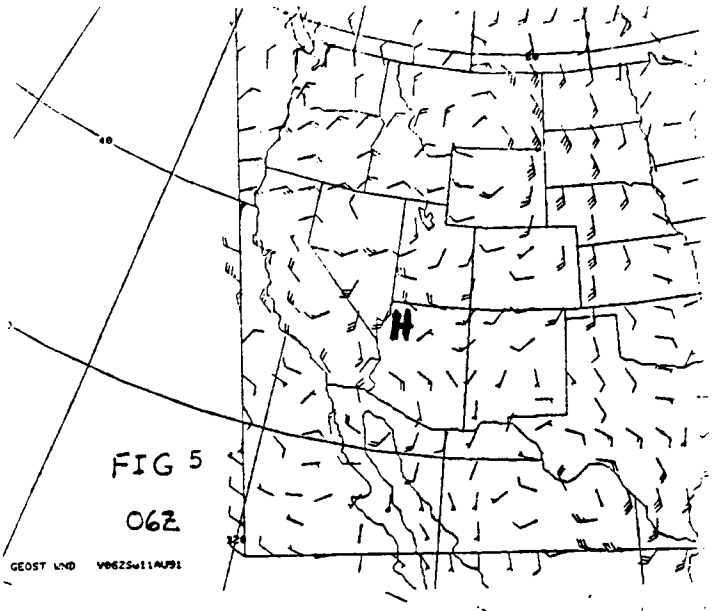


FIG 5

06Z

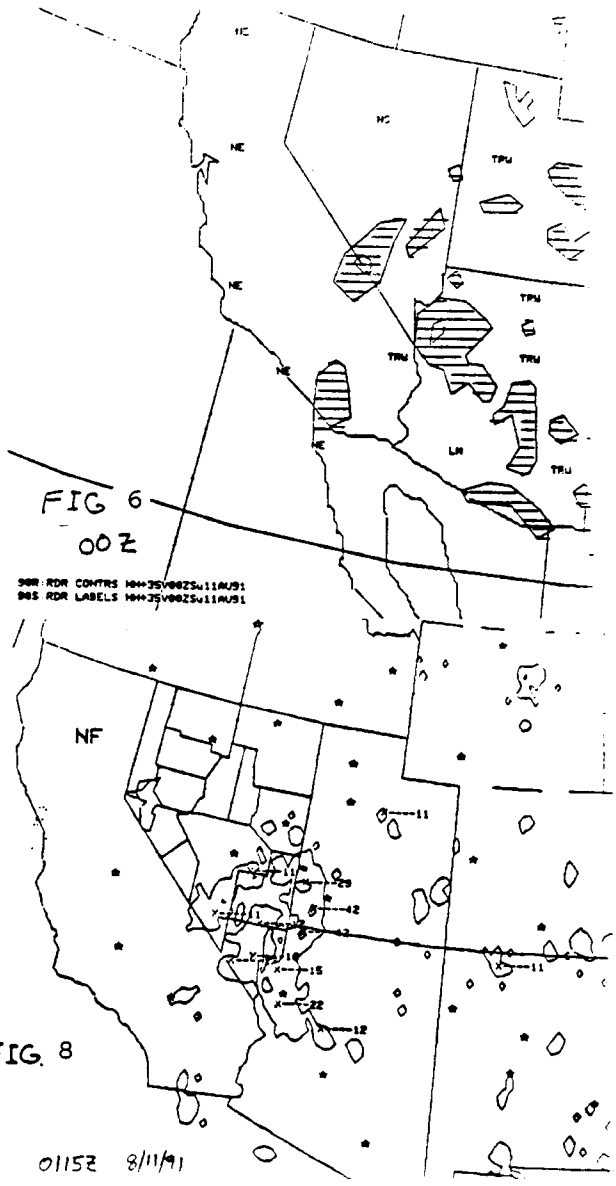


FIG 6

00Z

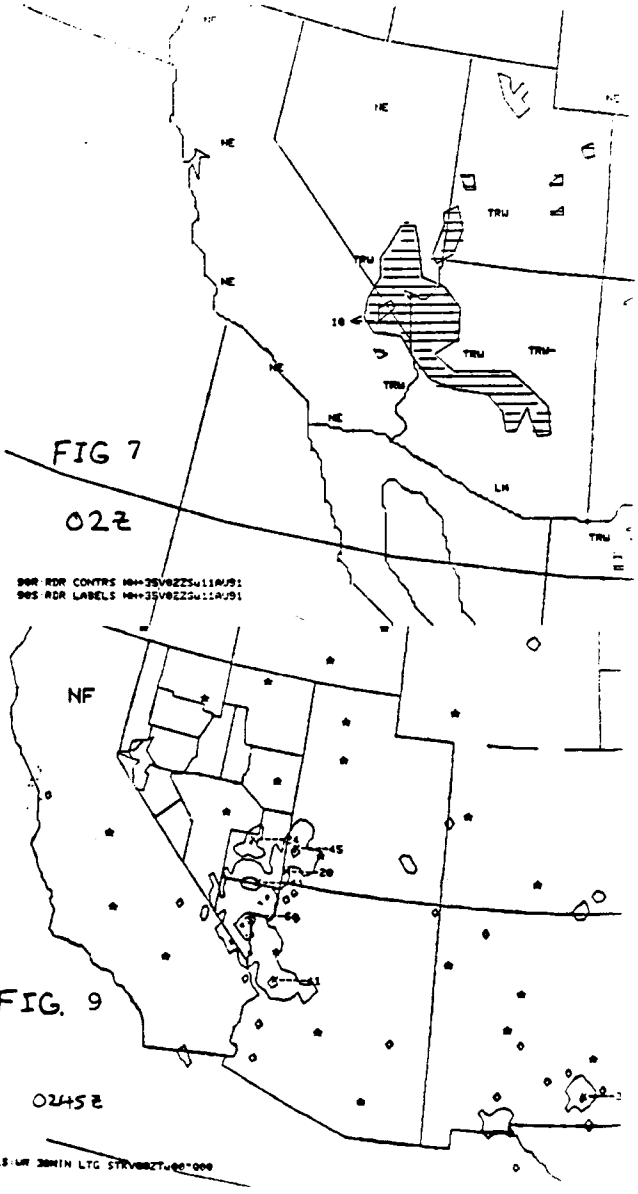


FIG 7

02Z

FIG. 8

FIG. 9

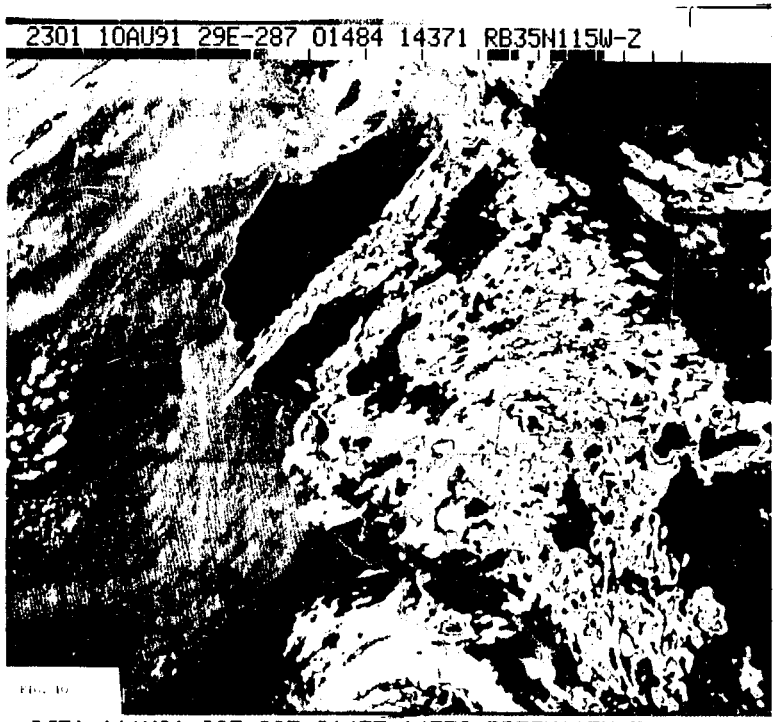
2301 10AU91 29E-287 01484 14371 RB35N115W-Z

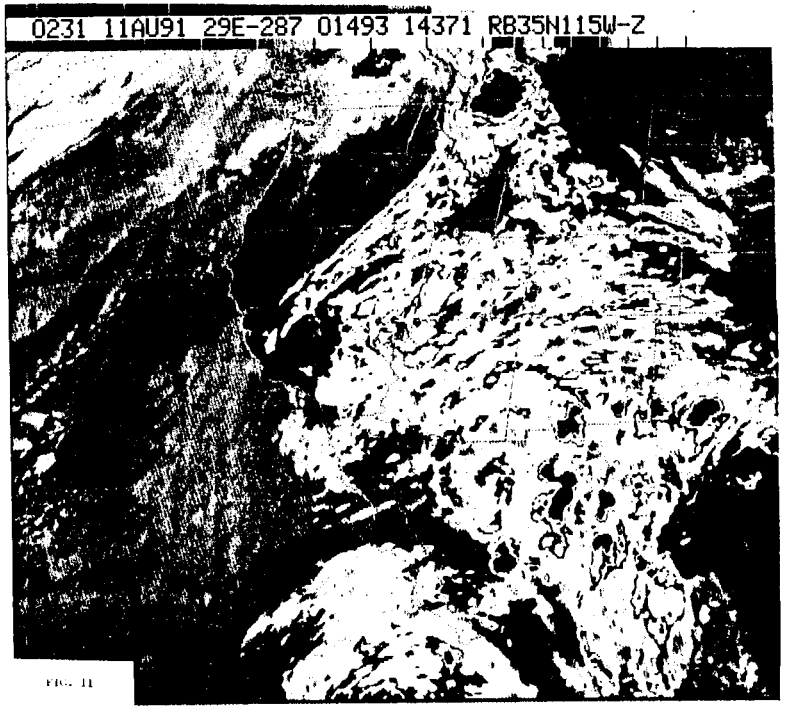
0231 11AU91 29E-287 01493 14371 RB35N115W-Z

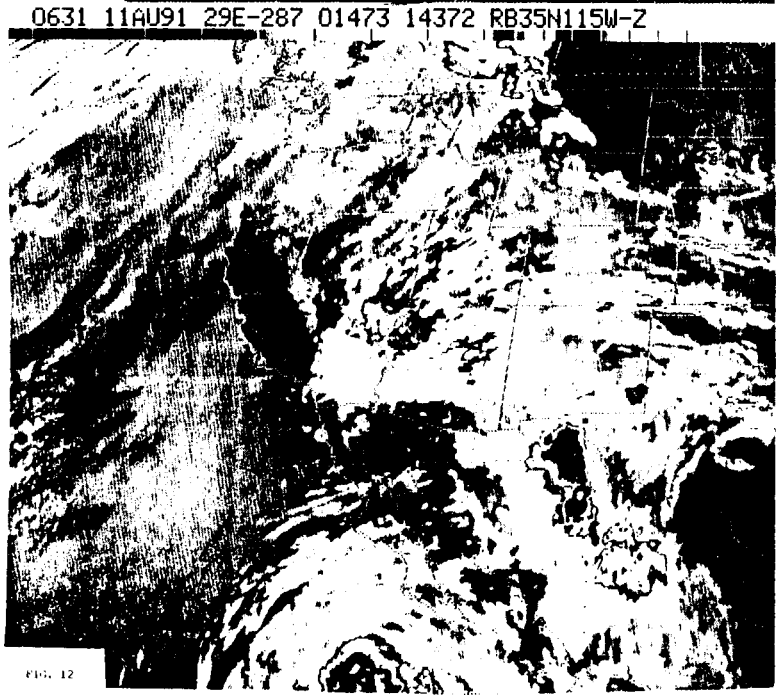
0631 11AU91 29E-287 01473 14372 RB35N115W-Z

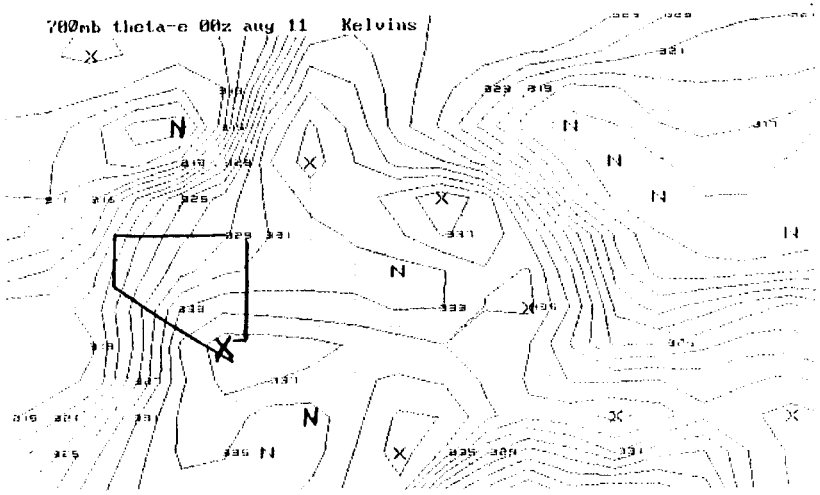
700mb theta-e 00z aug 11 Kelvins

FIG 13